DEUTSCHES ELEKTRONEN-SYNCHROTRON DESY

DESY SR-75/13
October 1975

Photoluminescence Excitation Spectra of Solid Krypton

by

Ch. Ackermann
Deutsches Elektronen-Synchrotron DESY, Hamburg

R. Brodmann, A. Suzuki, and G. Zimmerer
II. Institut für Experimentalphysik der Universität Hamburg

U. Hahn
Institut für Experimentalphysik der Universität Kiel

2 HAMBURG 52 · NOTKESTIEG 1

To be sure that your preprints are promptly included in the
HIGH ENERGY PHYSICS INDEX ,
send them to the following address (if possible by air mail) :

DESY
Bibliothek
2 Hamburg 52
Notkestieg 1
Germany

subject classification: 20.3; 23; 9

Photoluminescence Excitation Spectra of Solid Krypton

Ch. Ackermann, R. Brodmann[+], U. Hahn[++], A. Suzuki[+ 1)], and G. Zimmerer[+]

Deutsches Elektronen-Synchrotron DESY, Hamburg, Germany

[+]II. Institut für Experimentalphysik der Universität Hamburg, Hamburg, Germany

[++]Institut für Experimentalphysik der Universität Kiel, Kiel, Germany

---

1) On leave from Hitachi Central Laboratories, Tokyo, during July 1, 1974 to June 30, 1975

The excitation spectrum of the intrinsic photoluminescence of solid krypton has been investigated between 9.8 eV and 14 eV. Samples with a "clean" surface yield a quantum efficiency which is within an uncertainty of ~10 % independent of the kind of initially excited states. Surface contamination reduces the steady state concentration of excited states leading to quenching of the intrinsic luminescence. In the region of excitonic excitation the energy transfer between excitons and the surface is investigated. Assuming exciton diffusion, a diffusion length L_o = 200 Å is obtained for the n=1 and n'=1 excitons. Under the assumption of long range dipole dipole interaction a critical radius R_o = 22 Å is deduced.

Das Anregungsspektrum der intrinsischen Photolumineszenz von festem Krypton wurde zwischen 9,8 und 14 eV untersucht. Proben mit "reiner" Oberfläche zeigen, daß die Quantenausbeute mit einer Unsicherheit von 10 % unabhängig von der Art des angeregten Zustandes ist. Oberflächenkontamination verringert die stationäre Konzentration der angeregten Zustände, was zu einer Tilgung der intrinsischen Lumineszenz führt. Im Bereich der exzitonischen Anregungen wird der Energietransfer zwischen Exzitonen und der Oberfläche untersucht. Unter der Annahme von Exzitonendiffusion erhält man eine Diffusionslänge L_o = 200 Å für das n=1- und das n'=1-Exziton. Wenn man langreichweitige Dipol-Dipol-Wechselwirkung annimmt, ergibt sich ein kritischer Radius von 22 Å.

1. Introduction

The vacuum ultraviolet luminescence properties of solid Kr have been investigated for about ten years. Up to now, solid Kr has been excited by α-particles (1), electrons (2,3), x-rays (4), and by photons in the region of valence band excitations (5,6). In all of the investigations a broad luminescence band was found at about 8.25 eV. It is attributed to a Kr_2^* like luminescence center which can be created either via self-trapping of a free exciton or via self-trapping of a hole and additional capture of a free electron (7). It is similar to the luminescent center of the intrinsic luminescence of alkali halides (V_k + e^--center) (8). Whereas the intrinsic nature of the 8.25 eV band seems to be beyond doubt, it is not clear whether some other broad emission bands (see e.g. Ref. 4) are intrinsic or due to impurities.

Photoluminescence investigations are of special interest. Excitation by monochromatic light offers the advantage that the luminescent material is excited to definite states and that excitation spectra can be measured.

The already published excitation spectra of the 8.25 eV Kr band (5,6) cover the energetic region of excitonic absorption (the spin orbit split $\Gamma(3/2)$ and $\Gamma(1/2)$ exciton series) and the onset of interband transitions. Corresponding to each excitonic absorption maximum, a more or less deep minimum in the excitation spectrum is reported, indicating a reduced quantum efficiency. In the energetic region of low absorption coefficients maxima in the excitation spectra have been found. In the region of band to band transitions only a low luminescence efficiency was reported. The peculiar behaviour of the excitation spectra could not be explained satisfactorily up to now. In the region of excitonic excitation, similar effects

(like the deep minima) have also been reported in the case of other solid rare gases [9,10] and of alkali halides [11,12] There has been no convincing explanation, however.

In this paper, the excitation spectrum of the 8.25 eV Kr band is investigated in more detail. It will be shown that the peculiar structures of the excitation spectrum are mainly caused by surface contamination and that the quantum efficiency of pure solid Kr is approximately constant in the region of excitonic excitation. Even a slight contamination is able to quench the intrinsic luminescence. This quenching process is correlated to the absorption coefficient, α, and therefore to the penetration depth of light. Especially in the energetic region of the n=1 and n'=1 Kr excitons this quenching mechanism yields information about the transfer of excitation energy to the surface. It turns out that the shape of the excitation spectra can be explained under different assumptions; either diffusion of excitons to the surface or long range dipole-dipole interaction between immobile excitons and the contamination at the surface.

2. Experiment

The experiments were performed using the synchrotron radiation of the Deutsches Elektronen-Synchrotron DESY. The experimental set up is shown in Fig. 1. The synchrotron radiation was monochromatized by a near normal incidence monochromator (modified Wadsworth mounting [13]). The monochromatized light (band pass $\sim$8 Å) was focused onto the sample. The focus served as the entrance slit of a Seya Namioka monochromator with which the emitted light was analyzed (band pass $\sim$70 Å). The samples were prepared by condensation of Kr onto a gold coated sapphire plate mounted on a He cryostat. The Seya Namioka monochromator was attached to the sample chamber without a window. Both are designed for UHV-conditions. Because a replica grating was used, the Seya Namioka monochromator could not be baked. Typically a pressure of $\sim 10^{-9}$ Torr was obtained in the sample chamber.

Kr gas of a commercial purity of 99.9997 % (L'Air Liquide) was purified in a UHV gas inlet system by sputtering titanium. Within the sensitivity of the experiment, no extrinsic luminescence due to impurities could be observed. The thickness of the layers was controlled during evaporation by interference patterns of the reflectivity in the transparency region of Kr and ranged from 20.000 to 25.000 Å, providing total absorption for photon energies $\gtrsim$10 eV. The samples were prepared and investigaged at 5 K.

The luminescent light was converted by a sodium salicylate phosphor to the visible and detected by the usual photon counting techniques. Part of the exciting light was measured in the same way by aid of a reference monitor. The luminescence intensity signal of the 8.25 eV Kr band was divided electronically by the signal of the reference monitor and recorded with respect to the wavelength of the exciting light (excitation spectrum). In this way the characteristics of the light source, the near normal incidence monochromator, the focusing mirror, as well as the time fluctuations of the intensity of the synchrotron radiation are taken into account. However, the luminescence intensity is normalized by this procedure to the incident and not to the absorbed intensity.

At a background pressure of $\sim 10^{-9}$ Torr contamination cannot be neglected ($\sim$35 minutes for a monolayer of atomospheric gases [14]). Therefore the dependence of the excitation spectrum on time was measured. By extrapolating to time t=0 it was possible to get information about the spectra of layers with a "clean" surface.

3. Results

In Fig. 2, a set of excitation spectra of the 8.25 eV luminescence band of solid Kr at 5 K is presented. Curve I was measured immediately after

preparation of the sample, within 20 minutes. The curves II to V were obtained within the next 200 minutes. Each point of each curve can be correlated to a time scale beginning at the end of sample preparation. For the purpose of comparison, in Fig. 2 the absorption spectrum (Ref. 16) is included and the most important excitation energies of solid Kr are indicated (the $\Gamma(3/2)$ and $\Gamma(1/2)$ exciton series and the band gap, E_g).

The main features of the spectra are a sharp rise of luminescence intensity at about 9.85 eV, a maximum, A, at the low energy side of the n=1 exciton, followed by a minimum, M_1, which coincides with the n=1 exciton itself. Between the n=1 and n'=1 exciton, maximum B is found. It is followed by minimum M_1' which coincides with the n'=1 exciton. Towards higher excitation energies, the luminescence intensity increases again. The excitation spectrum shows a small dip M_2 at the energy of the n=2 exciton and smooth maxima at about 12 eV and 13.6 eV. The low energy tails of the spectra are due to excitation by higher order light of the near normal incidence monochromator.

The time development of the spectra from I to V shows a continuous decrease of luminescence intensity. The relative decrease is larger for the minima M_1, M_1' and M_2 than for the neighbouring maxima A,B,C. Therefore, the minima of the excitation spectra get more and more marked. Coinciding with the energy of the n=3 and n'=2 excitons, additional minima M_3 and M_2' appear. The luminescence intensity decreases considerably with time at high excitation energies.

In Fig. 3 the relative change of luminescence intensity, $(I(t)-I(o))/I(o)$, is plotted for different excitation energies versus the age, t, of the sample. The values of I(o) have been obtained by extrapolating the luminescence intensity, I(t), to t=o. The relative change is large for freshly evaporated

samples, until, apparently, 1 to 2 monolayers of contamination are grown. In Fig. 3 the time required to get 1 monolayer of atmospheric gases at a pressure of 10^{-9} Torr (14) is indicated. Later on the rate of change is smaller. The two curves given in Fig. 3 differ qualitatively by the absorption coefficient, α, for the different excitation energies. Whereas in the upper curve, the absorption coefficients are relatively large, they are an order of magnitude smaller for the lower curve (see e.g. Baldini's data given in Ref. 16). The only exception, of course, is the points for the low energy tail of the excitation spectra (9.7 eV) where the Kr layers are transparent. Because this low energy tail is caused by higher order light, it yields the behaviour for high absorption values. Measurements of the whole spectra with a LiF-filter suppressing higher orders were not possible because the LiF cutoff in combination with the monochromator characteristics allows measurements of the excitation spectra only below ~10 eV (intensity reasons). In the following figures for each spectrum a constant background given by the low energy tail is subtracted. Measurements of the excitation spectra of solid Xe (17) either with or without LiF-filter gives evidence that the error introduced by this procedure is tolerable in the region of the n=1 and n'=1 exciton.

4. Discussion

4.1 Excitation spectra of uncontaminated samples

In section 2 it was pointed out that the excitation spectra are normalized to the intensity of incident light and not to the intensity of absorbed light. This procedure is usually found in the literature. If the spectral dependence of the excitation spectrum (sample thickness d, quantum efficiency η, reflectivity R) is introduced exclusively by the spectral dependence of R and α, they fit the formula

$$Y = \eta(1-R)\cdot\left(1-\exp(-\alpha d)\right) \qquad (1)$$

In Fig. 4, the calculated excitation spectrum given by (1) and the experimental curve I of Fig. 2 are compared with each other. Additionally, at the energy of the maxima A,B,C and the minima M_1, M_1' the extrapolated luminescence intensities I(o) are indicated by crosses. For the calculation the reflectivity data on solid Kr given in Ref. 18 have been used. The calculated curve fits the extrapolated values nicely, as well as the measured curve I in the region of the n=1 and n'=1 excitons. The misfit at the A maximum (especially at its low energy side) is caused by the uncertainty in the knowledge of α-values for rare gases at the onset of absorption. We used the data of Ref. 16. These absorption data have a low energy tail extending to about 9.6 eV. For a Kr layer of about 20.000 Å thickness there would be total absorption down to at least 9.6 eV. The onset of the excitation spectrum, however, is found at 9.85 eV. The low energy tail in Baldini's Kr data, therefore, has been arbitrarily cut off around 9.8 eV for the purpose of this calculation. From such a procedure only a qualitative agreement between experiment and calculation can be expected in the region of maximum A.

From the overall agreement of the calculated curve and the measured curve I we conclude that the spectral dependence of the excitation spectrum of a freshly evaporated layer of Kr in the energy region of the n=1 and n'=1 excitons is mainly caused by the spectral dependence of the reflectivity. It follows that the quantum efficiency of such a layer is the same within 10 % for the n=1 and n'=1 exciton.

In Fig. 4, the experimental curve V from Fig. 2 is also included. The minima M_1 and M_1' of curve V cannot be explained by expression (1), because the relative decrease of luminescence intensity from curve I to curve V is different for the maxima and the minima, respectively. If the calculated curve is scaled down to the height of curve V at maximum B, the value of the calculated curve

in M_1 is higher by about a factor of 1.7, in M_1' by about a factor of 2.2 compared with measurement. Only reflectivity values of ∿70 % for the n=1 and n'=1 exciton as well can lead to a reasonable fit of curve V. For solid Kr, such high values of R can be excluded. The value of 50 % at the n=1 exciton given by Scharber and Webber (Ref.18) is an upper limit in the literature. In Ref. 19 only 30 % is reported.

4.2 Excitation spectra of Kr and exciton diffusion

At the onset of absorption the photoluminescence excitation spectrum of solid Kr is similar to the excitation spectrum of photoconductivity of semiconductors. The yield of photoconductivity of semiconductors sometimes has a pronounced maximum at the energy of the absorption edge. It drops to lower values if the absorption coefficient it high (and consequently the penetration depth of the exciting light is low) (20). This behaviour is explained by surface recombination of photogenerated carriers which gets important if the carriers are able to diffuse to the surface. Detailed model calculations for the photoconductivity yield including carrier diffusion have been performed by DeVore (21). DeVore's model has been successfully adopted in order to explain some features of the luminescence excitation spectra of semiconductors in the region of the absorption edge (22-24). Therefore we also adopt this model for the explanation of the excitation spectra of solid Kr in the excitonic region of absorption. The following assumptions are made:

(i) At the surface of the layers, excitons can recombine due to surface contamination. The surface recombination velocity, s, depends on the amount of contamination.

(ii) The excitons can move until they are self trapped. The motion of excitons is of a diffusive type.

The significance of the assumption of diffusive motion of excitons in solid rare gases has been discussed in detail in connection with several photoemission measurements on solid rare gases [25,26].

In analogy to DeVore's model, the spectral dependence of the ratio (luminescence intensity)/(incident intensity) is given by

$$Y = (1-R)\cdot(1/I_o)\cdot(1/\tau)\eta\cdot\int_o^d n(x)dx \qquad (2)$$

I_o is the incident intensity of exciting light, R is the reflectivity of the samples, τ is the lifetime of free excitons (limited by the self trapping process), η the quantum efficiency, n(x) is the steady state concentration of excitons at a distance x below the surface, and d is the thickness of the sample. Under steady state conditions n(x) is obtained as a solution of the diffusion equation

$$D\frac{d^2n}{dx^2} = \frac{n}{\tau} - I_o\cdot\alpha\cdot\exp(-\alpha x) \qquad (3)$$

(D: diffusion coefficient of free excitons). The influence of the surface is introduced by the boundary conditions

$$-D\left(\frac{dn}{dx}\right)_{x=0} = -n(0)\cdot s \qquad (4a)$$

$$D\left(\frac{dn}{dx}\right)_{x=d} = -n(d)\cdot s^* \qquad (4b)$$

(s, s^*: surface recombination velocity at the front and at the back, respectively). Because we used thick films ($d >> 1/\alpha$), the value of s^* is not important for our calculation.

From $\int_o^d n(x)dx$ introduced in (2) the excitation spectrum can be calculated. With s=0 eq. (2) turns into eq. (1). The expression for $\int_o^d n(x)dx$ contains two unknown quantities: the diffusion length $L_o = \sqrt{D\cdot\tau}$ of free excitons and the ratio s/v_d, where v_d means the diffusion velocity L_o/τ. These quantities can

be obtained from a fit of the calculated curve to the measured curve. The excitation spectra are calculated in relative units since the quantum efficiency η is unknown.

In Fig. 5 it is demonstrated that calculated excitation spectra with L_o=200 Å and variable s/v_d qualitatively explain the set of measured excitation spectra. The upper curve with s/v_d=0 represents the same plot as in Fig. 4 according to eq. (1). With increasing values of s, the minima M_1 and M_1' get more and more marked. With $s/v_d \gtrsim 100$ the calculated curves get independent of the choice of s/v_d. From the measurements it is also found that the excitation spectra approach a static curve more and more with increasing contamination (curve V of Fig. 2).

In Fig. 6, therefore a model curve with s/v_d = 100 is compared with curve V of Fig. 2. The diffusion length of the excitons was used as fitting parameter. The absolute value of the calculated curve has not been fitted to the measured curve. It is consistent with the fit of Fig. 4, where the measured curve I has been fitted with s/v_d=0. The calculated curve in Fig. 6 describes the overall decrease of the excitation spectra by surface quenching as well as the pronounced minima M_1 and M_1'. The best fit is obtained with $L_o \approx 200$ Å. The result of Fig. 6 indicates that both the n=1 and n'=1 excitons are described by approximately the same diffusion length L_o.

The value of L_o obtained by such a fit depends sensitively on the absolute value of α used in the calculation. We used $\alpha = 1.6 \cdot 10^6$ cm^{-1} at the n=1 exciton. This value was taken from Ref. 16 and seems to be consistent with the corresponding values of other rare gases given in Ref. 16. However, in Ref. 18, for the n=1 exciton, an absorption coefficient $\alpha = 6 \cdot 10^5$ cm^{-1} is given. Using this value results in a diffusion length of ~600 Å. The value of L_o=200 Å is close

to the diffusion length of exciton in solid Xe (160-300 Å) and Ar (120 Å) which are given in Ref. 26 and which are supported by theoretical consideration [25,26].

The diffusion model for free excitons of Ref. 25 and the model used here only differ in the boundary conditions. In Ref. 25, $n(0)=0$ was used and the existence of a "dead layer" was discussed. The boundary condition $\frac{dn}{dx} = 0$ at the surface was ruled out explicitly. Eq. (4a,b) include both possibilities discussed in Ref. 25. With $s=0$, $\frac{dn}{dx} = 0$ at the surface is obtained, and with $s\to\infty$, $n(0)\to 0$ is reached. The influence of s on n(0) is obtained from n(x) in the case of infinite thickness of the layers (in our case, apart from the onset of absorption, the thickness of the layers is always much larger than the penetration depth of light):

$$n(0) = \frac{I_o \alpha \tau}{\alpha L_o + 1} \quad \frac{1}{1+s/v_d} \tag{5}$$

From Fig. 5 it is seen that rather small values of s/v_d ($\sim$1) already influence the shape of the excitation spectra drastically. n(0) is reduced by about 50 % when s/v_d changes from $s/v_d=0$ to $s/v_d=1$, but no indication of a "dead layer" is obtained. Only some hours after preparation a state with $s/v_d=100$ is reached and n(0) reduced to $\sim$1 %. In this case one can talk about a "dead layer" for free excition near the surface and the bondary condition $n(0)=0$ is a good approximation.

The photoluminescence excitation spectrum of a "clean" Kr layer cannot be explained by assuming the boundary condition $n(0)=0$. Within the sensitivity of the experiment it can be explained by $s=0$ that is $D \cdot \frac{dn}{dx} = 0$ at the surface.

4.3 Excitation spectra of Kr and long range dipole-dipole interaction

In this model, it is assumed that immobile excitons are able to transfer their energy to contamination atoms or molecules at the surface of the samples

via dipole-dipole interaction. The interaction strength is characterized by a critical radius R_o according to Förster's theory [27]. Neglecting effects at the back of the layers ($d \gg \frac{1}{\alpha}$), the equilibrium between generation and decay of excitons is given by

$$I_o \, \alpha \exp(-\alpha x) = \frac{n(x)}{\tau} + \frac{n(x)}{\tau} \cdot \sum_{\ell(\text{surface})} (R_o/R_\ell)^6 \qquad (6)$$

R_ℓ denotes the distance exciton - surface atom at site ℓ. Assuming a homogeneous layer of contamination (characterized by a number of a atoms/cm^2) the sum in eq. (6) can be calculated:

$$\sum_\ell \left(\frac{R_o}{R_\ell}\right)^6 = \int_0^\infty a \cdot \frac{R_o^6}{(x^2+r^2)^3} \, 2\pi r dr = \frac{\pi}{2} \, \frac{R_o^6 a}{x^4} \qquad (7)$$

Only the first monolayer of contamination is taken into account. We set $\frac{\pi}{2} R_o^6 \cdot a = d_o^4$. The solution of eq. (6) is

$$n(x) = I_o \alpha \exp(-\alpha x) \cdot \tau \cdot \frac{1}{1+d_o^4/x^4} \qquad (8)$$

The quantity d_o can be regarded as the thickness of a "dead layer" for excitons. For $d_o \neq 0$, $n(0)=0$. In the region of $x \approx d_o$, $n(x)$ has a sharp increase, and with $x \gg d_o$ approximately the concentration $n(x)$ given by generation is reached.

In Fig. 7 a set of calculated excitation spectra is given with different values of d_o as a parameter. With $d_o = 0$ (equivalent to $a=0$) the case of a clean sample is described (no energy transfer). Increasing values of d_o describe increasing influence of surface contamination. Qualitatively the set of surves of Fig. 7 resembles very much the set of curves obtained from the diffusion model already presented in Fig. 5.

In Fig. 8 the same experimental curve as in Fig. 6 is compared with a calculated curve. The height of both spectra is consistent with the height of the curves of "clean" Kr because experiment and calculation are fitted one to each other only in the case of $d_o=0$. From Fig. 8, $d_o=80$ AE is obtained. Within the experimental uncertainties both the fit of Fig. 6 and the fit of Fig. 8 are quite similar.

From the value of d_o, with a reasonable assumption of $a=2{,}5\times10^{15}$ atoms/cm^2 (1 atom per 2x2 Å^2) for a contaminated surface and a critical radius $R_o\approx22$ Å is obtained. This value is in rough agreement with $R_o=17$ Å calculated according to Ref. 27.

We want to state that there is a great difference between the models in describing the losses at the surface. In the diffusion model, losses occur only during the time when the excitons are free, that is $\sim10^{-11}$-10^{-12} sec, while in the dipole model energy transfer occurs during the whole radiative lifetime of the exciton, that is $\sim10^{-9}$ sec.

4.4 Region of higher excitation energies

The increase of the excitation spectra at about 11 eV seems to indicate an increase of γ for the higher members of the exciton series as well as the band to band excitations. However, this is doubtful for the following reason: preliminary measurements of the excitation spectra at higher excitation energies indicate that in solid Kr electron-electron scattering drastically enhances the luminescence yield (28). The onset of electron-electron scattering obviously takes place at an excitation energy $E=E_g+E(n=1)$ where $E(n=1)$ denotes the energy of the n=1 exciton. In the second order spectrum of the monochromator this energy coincides with the measured increase of luminescence at about 11 eV. The increase is of the same size as the low energy tail which

were explained by second order effects of the spectrum. Second order light is also responsible for the increase of luminescence intensity at 11 eV.

The weak structures of the excitation spectra above 12 eV seem to be caused by the spectral dependence of R. Especially the minimum at 12.7 eV nearly coincides with the reflectivity maximum at 12.8 eV [21]. The decrease of luminescence intensity above 13.6 eV coincides with the increase of reflectivity to a maximum at 14.2 eV [21]. Therefore, for "clean" Kr samples an approximately constant η in the whole range of energy covered by our experiment is indicated.

5. Concluding Remarks

From the point of view of photoluminescence it is an open question whether exciton diffusion or long range dipole-dipole interaction is dominant for energy transfer in solid Kr. In other molecular solids like organic crystals it is also not clear whether exciton diffusion or dipole-dipole interaction is dominant [29]. In the case of rare gases, however, photoemission measurements support the assumption of exciton diffusion [25,26].

It is unclear why the application of the diffusion model to photoluminescence and photoemission is only possible with different boundary conditions for the concentration of free excitons.

Probably the two experimental methods don't measure the same kind of "free excitons". There is a contribution to photoemission only from those "free excitons" which lead to a free electron with an energy above the vacuum level via one of the processes discussed in Ref. 25, whereas photoluminescence is sensitive also for those excitons which are lost for photoemission but still can move.

It is not yet known whether quenching of the intrinsic luminescence at the surface of Kr is non radiative or leads to some extrinsic emission. In the case of Xe, Huber et al. (2) found out that a certain extrinsic luminescence band was correlated to the partial pressure of O_2 in the background pressure of their system. We have not yet found similar effects within the sensitivity of our experiment.

Finally it may be pointed out that the properties of the Kr excitation spectra seem to be representative also for solid Ar and solid Xe. The excitation spectra of Ar and Xe of Ref. 5 and 10 can now be explained by surface recombination of free exctions. In the case of samples with a "clean" surface, similar results are obtained as with solid Kr (30).

Acknowledgement

We would like to thank Prof. R. Haensel for his stimulating interest and support of this work and Dr. N. Schwentner for helpful discussions. Thanks are due to the Bundesminsterium für Forschung und Technologie for financial support.

References

1. A. Gedanken, B. Raz, and J. Jortner, J.Chem.Phys. 59, 5471 (1973)
2. N.G. Basov, E.M. Balashov, O.V. Bogdankevitch, V.A. Danilychef, G.N. Kashnikov, N.P. Lantzov, and D.D. Khodkevitch, J. Luminescence 1, 834 (1970) E.E. Huber, Jr., D.A. Emmons, and R.M. Lerner, Optics Commun. 11, 155 (1974)
3. A. Bonnot, A.M. Bonnot, F. Coletti, J.M. Debever et J. Hanus, Journal de Physique 35, C3-49 (1974)
4. M. Creuzburg, Solid State Communic. 9, 665 (1971)
5. R. Brodmann, R. Haensel, U. Hahn, U. Nielsen, and G. Zimmerer, in Vacuum Ultraviolet Radiation Physics, edited by E.E. Koch, R. Haensel, and C. Kunz (Vieweg/Pergamon, Braunschweig 1974) p. 344
6. N. Nagasawa and T. Nanba, Optics Commun. 11, 152 (1974)
7. M. Martin, J.Chem.Phys. 54, 3289 (1971)
8. M.N. Kabler and D.A. Patterson, Phys.Rev.Lett. 19, 652 (1967)
9. T. Nanba and N. Nagasawa, J.Phys.Soc. Japan 36, 1216 (1974)
10. R. Brodmann, R. Haensel, U. Hahn, U. Nielsen, and G. Zimmerer, Chem.Phys.Lett. 29, 250 (1974)
11. J. Ramamurti and K. Teegarden, Phys.Rev. 145, 698 (1966)
12. M. Ikezawa and T. Kojima, J.Phys.Soc. Japan 27, 1551 (1969)
13. M. Skibowski and W. Steinmann, J.Opt.Soc.Am. 57, 112 (1967)
14. G. Lewin, Fundamentals of Vacuum Science and Technology, McGraw Hill Book Company, New York (1965)
15. B. Sonntag, in Rare Gas Solids, edited by M.L. Klein and J.A. Venables (Academic Press, 1975) to be published
16. G. Baldini, Phys.Rev. 128, 1562 (1962)
17. G. Tolkiehn, Diplomarbeit, Universität Hamburg, 1975
18. S.R. Scharber, Jr. and S.E. Webber, J.Chem.Phys. 55, 3985 (1971)
19. R. Haensel, G. Keitel, E.E. Koch, M. Skibowski and P. Schreiber, Opt. Commun. 2, 59 (1970)

20. see e.g. R.H. Bube, Photoconductivity of Solids, J. Wiley & Sons, Inc., New York (1960) and references given therein

21. H.B. DeVore, Phys.Rev. 102, 86 (1956)

22. J. Vilms and W.E. Spicer, J.Appl.Phys. 36, 2815 (1965)

23. M. Gershenzon and R.M. Mikulyak, Appl.Phys.Lett. 8, 245 (1966)

24. P.J. Dean, Phys.Rev. 168, 889 (1968)

25. Z. Ophir, B. Raz, J. Jortner, V. Saile, N. Schwentner, E.E. Koch, M. Skibowski, and W. Steinmann, J.Chem.Phys. 62, 650 (1975)

26. J. Jortner, in Vacuum Ultraviolet Radiation Physics, edited by E.E. Koch, R. Haensel, and C. Kunz, (Vieweg/Pergamon, 1974) p. 263

27. Th. Förster, Annalen der Physik 2, 55 (1948)

28. Ch. Ackermann, R. Brodmann, U. Hahn, H. Möller, and G. Zimmerer, to be published

29. a) O. Simpson, Proc.Roy.Soc. A 238, 402 (1957)
b) R.C. Powell, Phys.Rev. B 2, 1159 (1970) and references therein

30. Ch. Ackermann, R. Brodmann, R. Haensel, U. Hahn,G. Tolkiehn, and G. Zimmerer, Proceedings of the Intern. Conf. on Luminescence, Tokyo (1975), to be published

Figure Captions

Fig. 1 Experimental set up (P.M.: photo multiplier)

Fig. 2 Excitation spectra of the 8.25 eV Kr luminescence band at 5 K. The absorption spectrum of solid Kr at the top is taken from Ref. 16

Fig. 3 Relative decrease of luminescence intensity due to surface contamination for different excitation energies.

Fig. 4 Comparison of measured excitation spectra I and V with a calculation according to eq. (1). Curve I: Kr layer with a nearly "clean" surface. Curve V: contaminated Kr layer. The crosses give extrapolated values I(o)

Fig. 5 Calculated excitation spectra of Kr (diffusion model)

Fig. 6 Comparison between excitation spectrum V (solid line) and model calculation (diffusion model)

Fig. 7 Calculated excitation spectra of Kr (dipole-dipole energy transfer model)

Fig. 8 Comparison between excitation spectrum V (solid line) and model calculation (dipole-dipole energy transfer model)

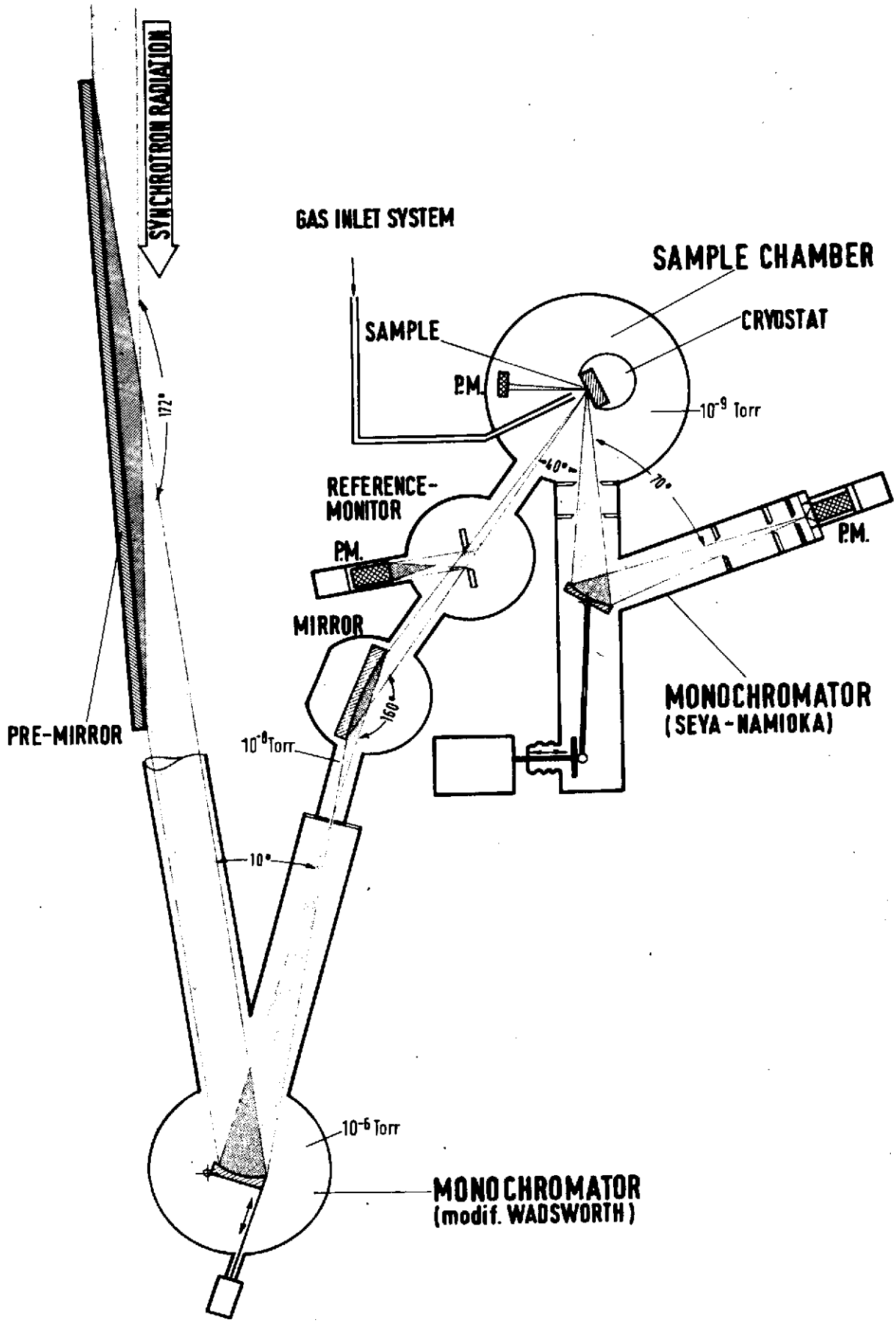
SYNCHROTRON RADIATION
GAS INLET SYSTEM
SAMPLE CHAMBER
SAMPLE
CRYOSTAT
P.M.
10^{-9} Torr
172°
40°
70°
REFERENCE-
MONITOR
P.M.
P.M.
MIRROR
160°
MONOCHROMATOR
(SEYA-NAMIOKA)
PRE-MIRROR
10^{-8} Torr
10°
10^{-6} Torr
MONOCHROMATOR
(modif. WADSWORTH)

Fig. 1

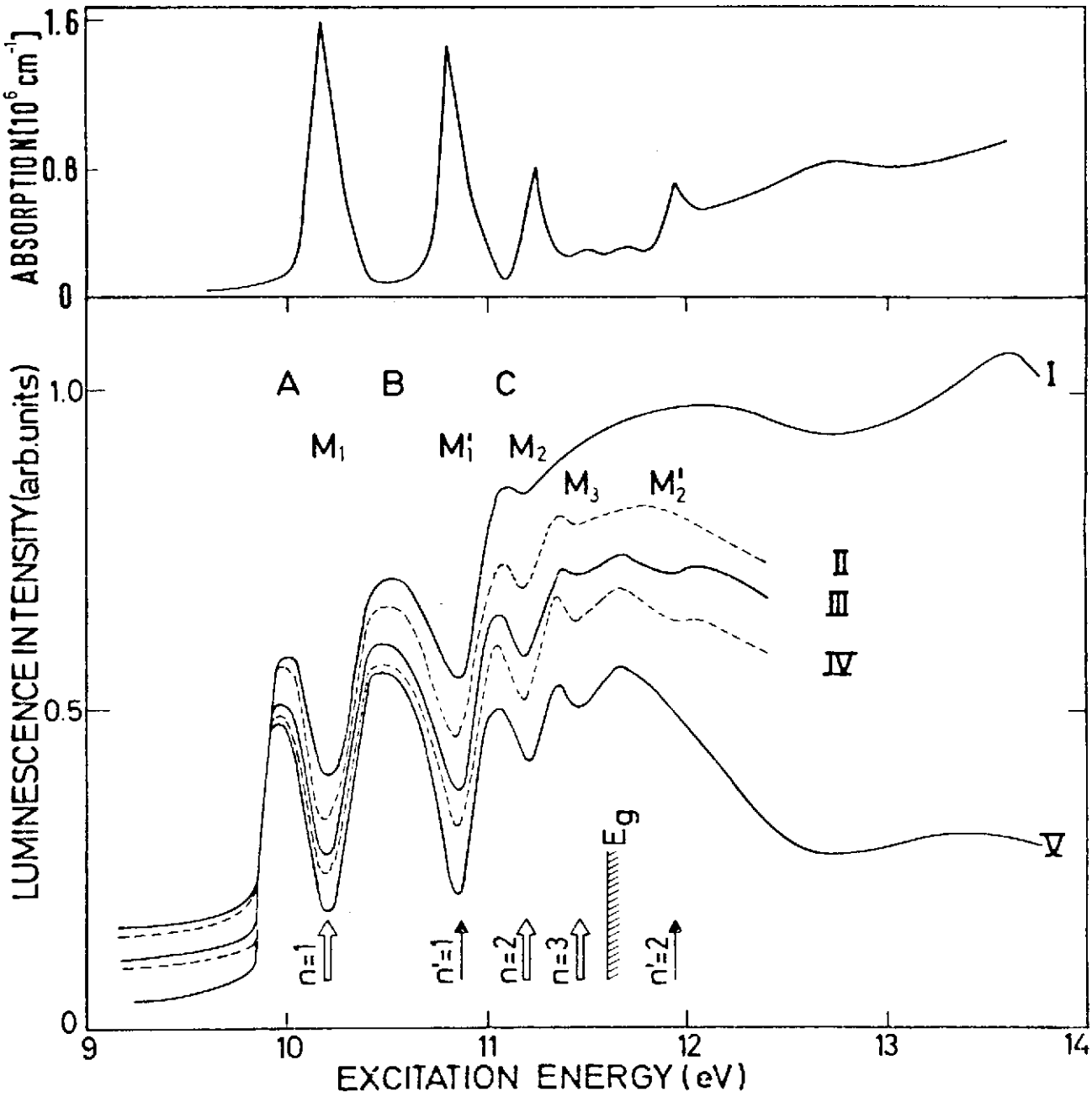
ABSORPTION(10^6 cm^-1)
1.6
0.8
0
LUMINESCENCE INTENSITY(arb.units)
1.0
0.5
0
A
B
C
M1
M'1
M2
M3
M'2
I
II
III
IV
V
Eg
n=1
n'=1
n=2
n=3
n'=2
9
10
11
12
13
14
EXCITATION ENERGY (eV)

Fig. 2

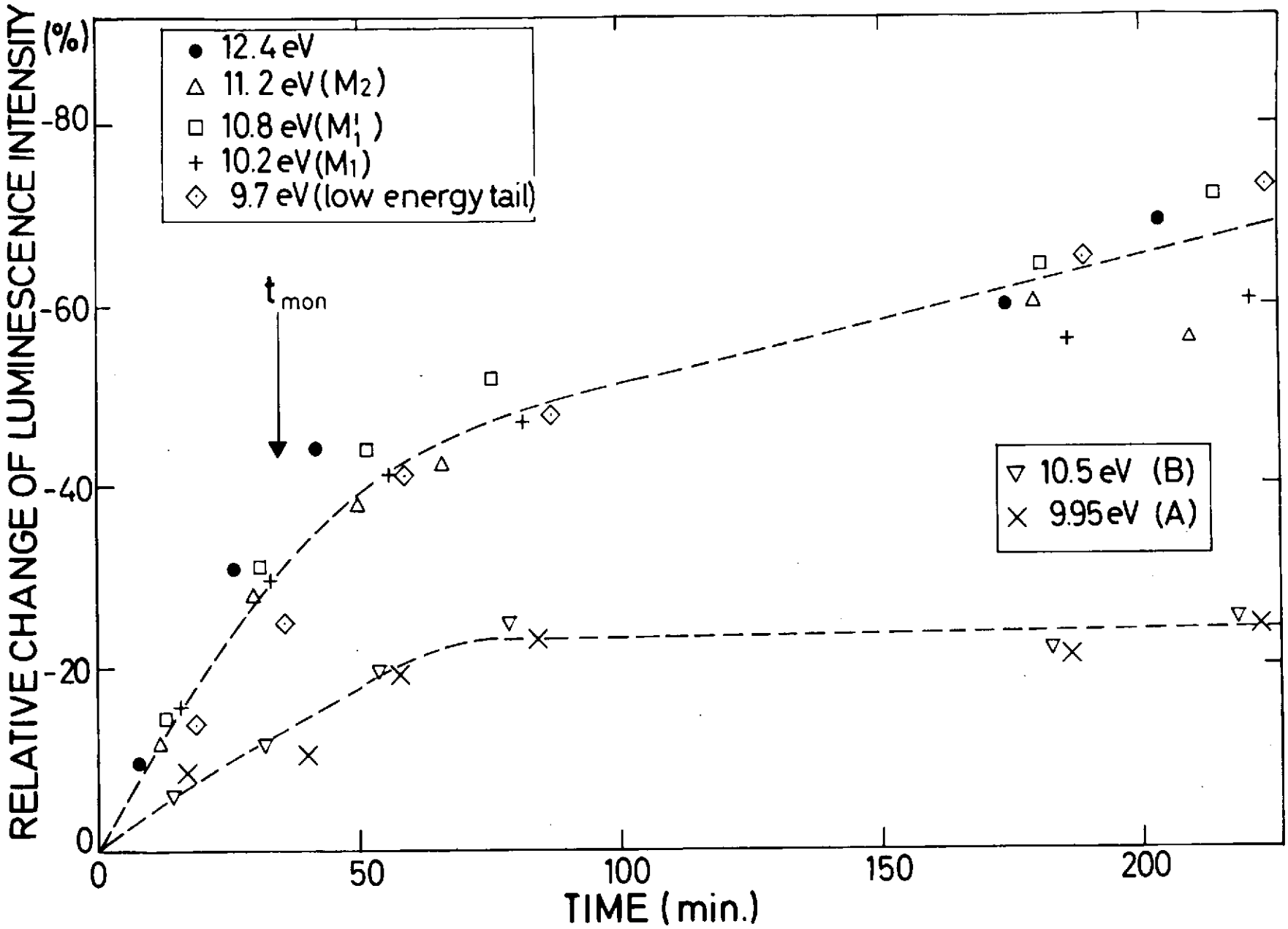
RELATIVE CHANGE OF LUMINESCENCE INTENSITY (%)
0
-20
-40
-60
-80
0
50
100
150
200
TIME (min.)
12.4 eV
11.2 eV (M2)
10.8 eV (M1')
10.2 eV (M1)
9.7 eV (low energy tail)
t mon
10.5 eV (B)
9.95 eV (A)

Fig. 3

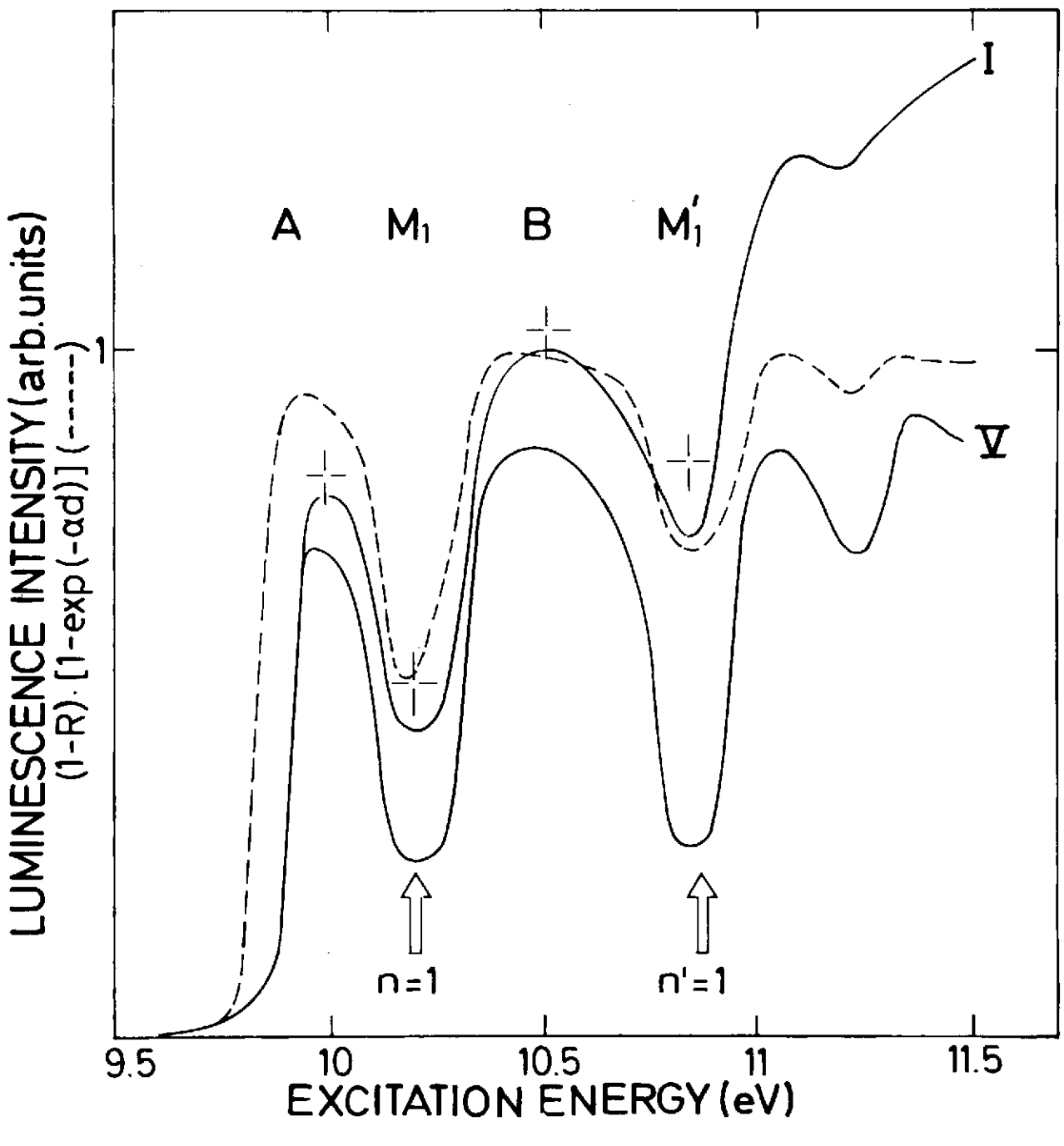
LUMINESCENCE INTENSITY(arb.units)
(1-R)·[1-exp(-αd)] (-----)
1
A
M1
B
M'1
I
V
n=1
n'=1
9.5
10
10.5
11
11.5
EXCITATION ENERGY (eV)

Fig. 4

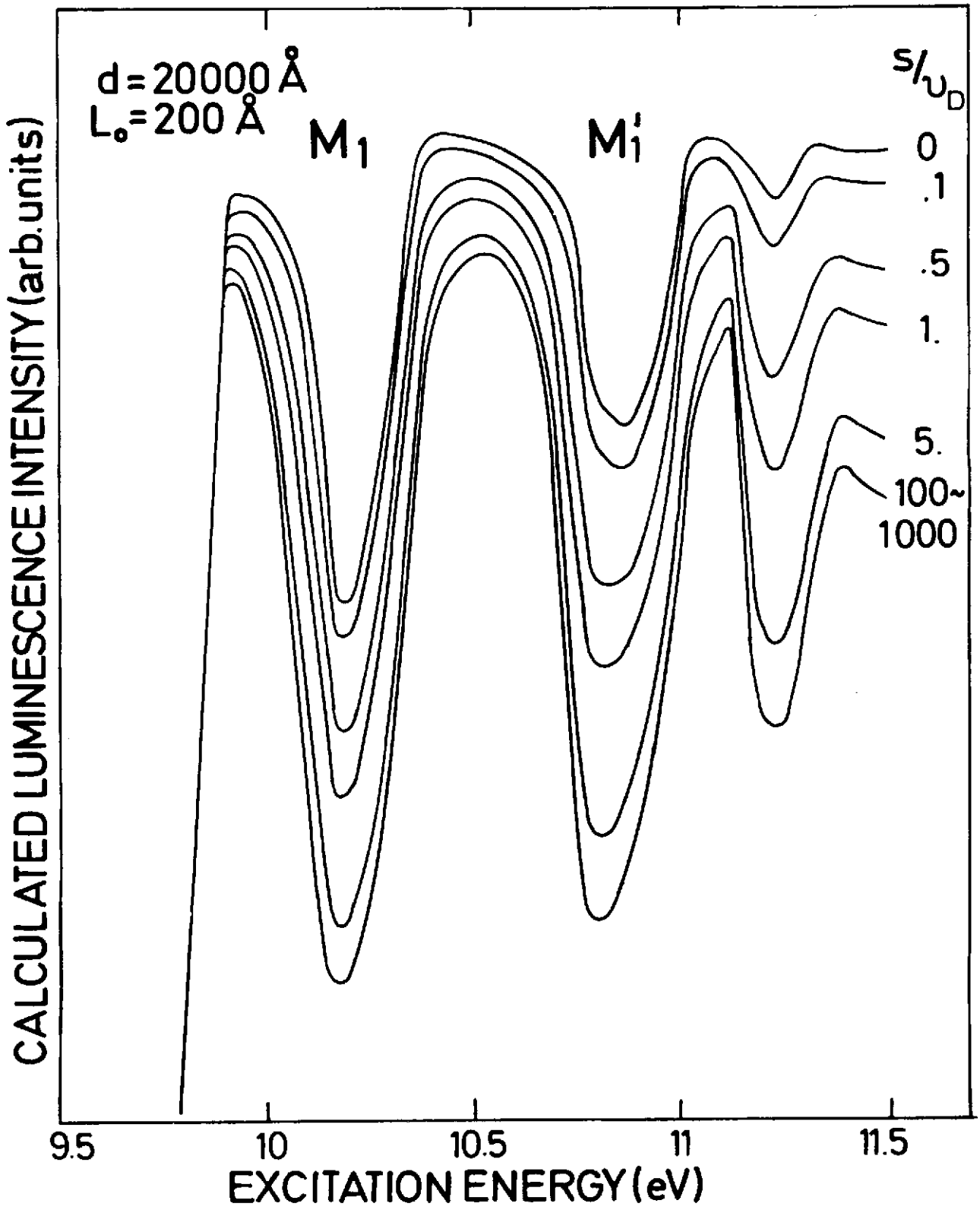
d = 20000 Å
L₀ = 200 Å
M1
M1'
S/UD
0
.1
.5
1.
5.
100~
1000
CALCULATED LUMINESCENCE INTENSITY (arb.units)
9.5
10
10.5
11
11.5
EXCITATION ENERGY (eV)

Fig. 5

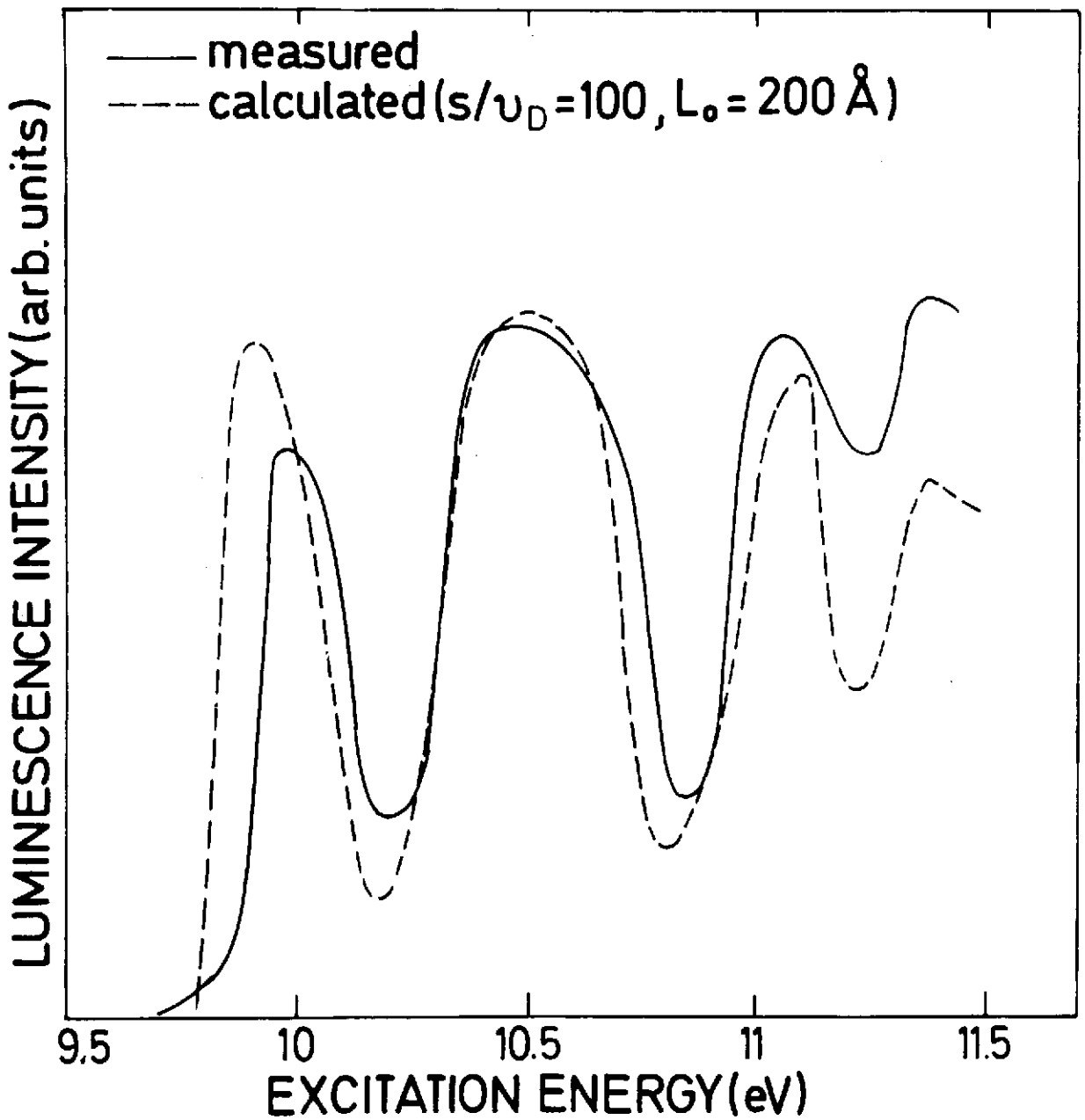
measured
calculated (s/υD = 100, L₀ = 200 Å)
LUMINESCENCE INTENSITY (arb. units)
9.5
10
10.5
11
11.5
EXCITATION ENERGY (eV)

Fig. 6

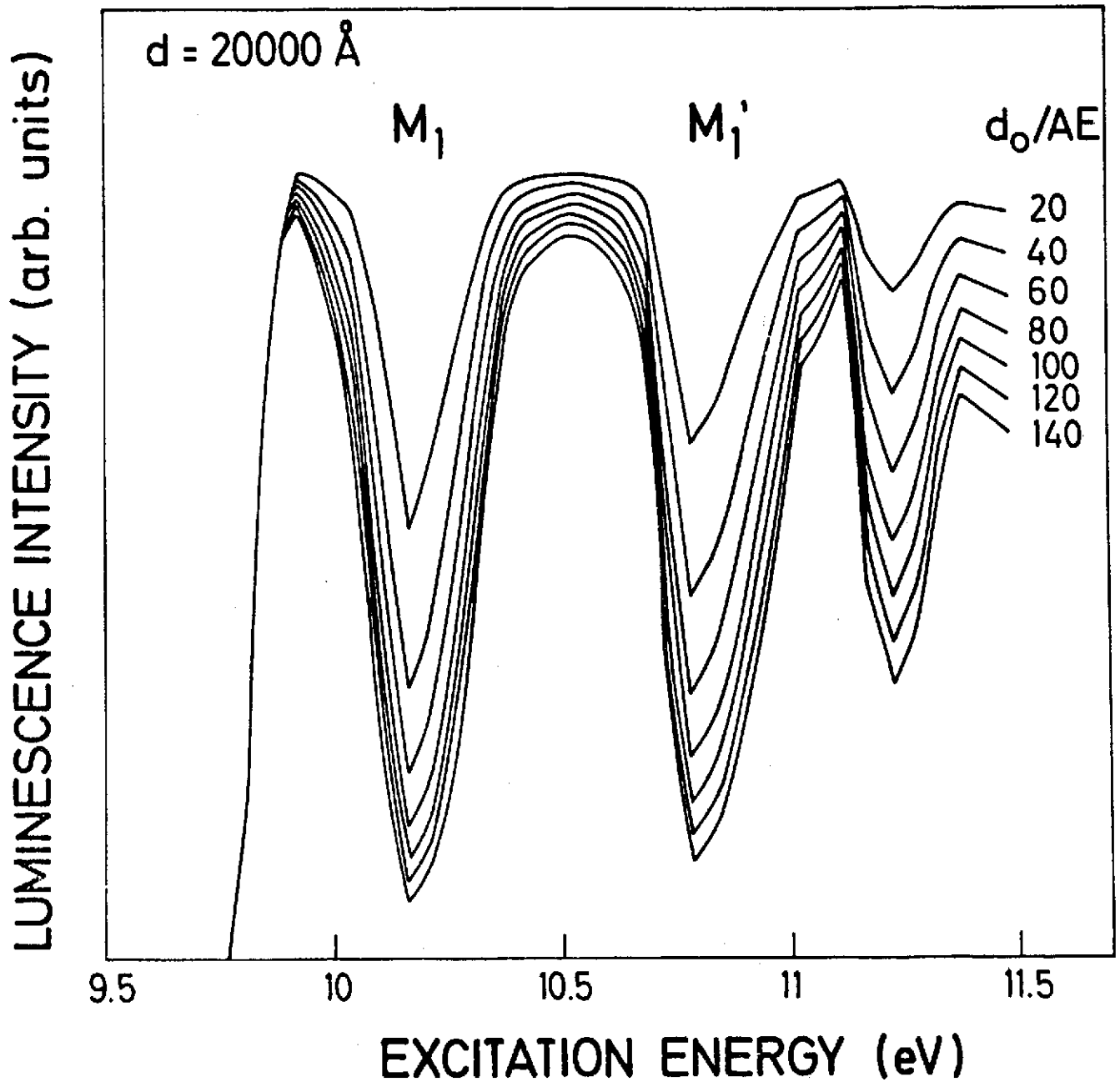
d = 20000 Å
M1
M1'
do/AE
20
40
60
80
100
120
140
LUMINESCENCE INTENSITY (arb. units)
9.5
10
10.5
11
11.5
EXCITATION ENERGY (eV)

FIG. 7

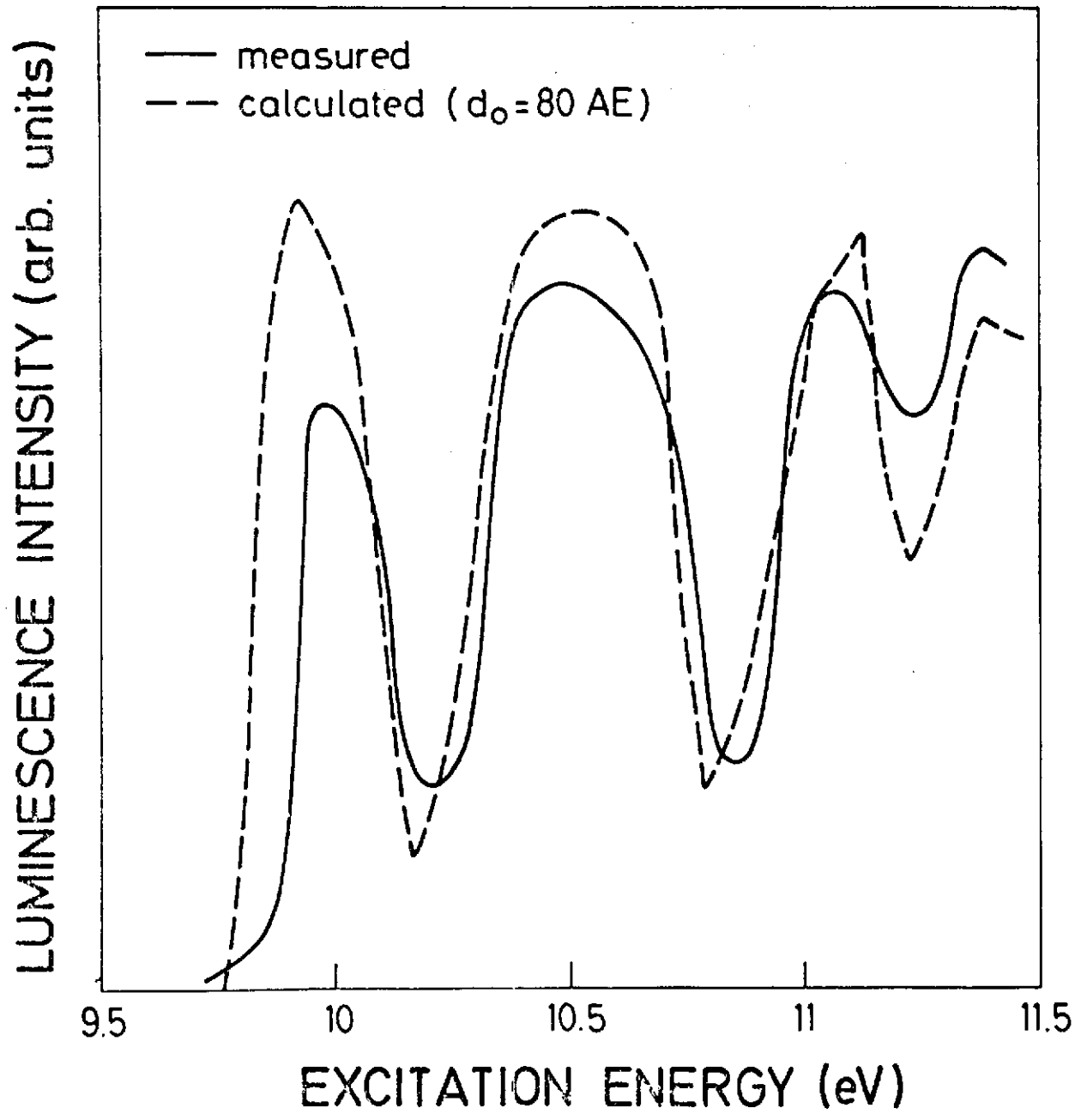
measured
calculated (d_o=80 AE)
LUMINESCENCE INTENSITY (arb. units)
9.5
10
10.5
11
11.5
EXCITATION ENERGY (eV)

Fig. 8